Published in final edited form as:
Eur J Neurosci. 2008 April ; 27(7): 1686–1699. doi:10.1111/j.1460-9568.2008.06141.x.

Unique clustering of A-type potassium channels on different cell types of the main olfactory bulb

Mihaly Kollo[*], **Noémi Holderith**[*], **Miklós Antal**, and **Zoltan Nusser**
Laboratory of Cellular Neurophysiology, Institute of Experimental Medicine, Budapest, HUNGARY

Abstract

Theoretical and functional studies predicted a highly non-uniform distribution of voltage-gated ion channels on the neuronal surface. This was confirmed by recent immunolocalization experiments for Na^+, Ca^{2+}, HCN and K^+ channels. These experiments also indicated that some K^+ channels were clustered in synaptic or non-synaptic membrane specializations. Here we analyzed the subcellular distribution of Kv4.2 and Kv4.3 subunits in the rat main olfactory bulb at high resolution to address whether clustering characterizes their distribution and whether they are concentrated in synaptic or non-synaptic junctions. The cell surface distribution of the Kv4.2 and Kv4.3 subunits is highly non-uniform. Strong Kv4.2 subunit immunopositive clusters were detected in intercellular junctions made by mitral, external tufted and granule cells. We also found Kv4.3 subunit immunopositive clusters in periglomerular (PGC), deep short-axon and granule cells. In the juxtaglomerular region some calretinin immunopositive glial cells enwrap neighboring PGC somata in a cap-like manner. Kv4.3 subunit clusters are present in the cap membrane that directly contacts the PGC, but not the one that faces the neuropil. In membrane specializations established by members of the same cell type, K^+ channels are enriched in both membranes, whereas specializations between different cell types contain a high density of channels asymmetrically. None of the K^+ channel-rich junctions showed any of the ultrastructural features of known chemical synapses. Our study provides evidence for highly non-uniform subcellular distributions of A-type K^+ channels and predicts their involvements in novel forms of intercellular communication in the olfactory pathway.

Keywords

voltage-gated K^+ channels; immunohistochemistry; olfactory bulb; microcircuit

Introduction

Voltage-gated ion channels play a key role in determining how excitable cells integrate and generate electrical signals. Electrophysiological and immunohistochemical studies examining the cell surface distribution of these channels revealed that neurons express specific subsets and densities of ion channels in different subcellular compartments. For example, distinct Na^+ channel subtypes were found in different parts of the axonal and somato-dendritic membrane of neurons (Rasband *et al.*, 1999; Boiko *et al.*, 2001; Jenkins & Bennett, 2001; reviewed by Trimmer & Rhodes, 2004). An uneven cell surface distribution of Ca^{2+} (Kulik *et al.*, 2004; Obermair *et al.*, 2004) and hyperpolarization activated mixed

Correspondence to: Zoltan Nusser Laboratory of Cellular Neurophysiology, Institute of Experimental Medicine, Hungarian Academy of Sciences, Szigony Street 43 1083 Budapest, HUNGARY Tel.: 36 1 210 9983 Fax: 36 1 210 9984 e-mail: nusser@koki.hu.
[*]These authors contributed equally to this work.

Europe PMC Funders Author Manuscripts

cation (HCN; Santoro *et al.*, 1997; Lorincz *et al.*, 2002; Notomi & Shigemoto, 2004; Lujan *et al.*, 2005) channels has also been demonstrated.

Among voltage-gated ion channels, K^+ channels have received special attention due to their extraordinary molecular diversity and susceptibility to many forms of modification (reviewed by Gutman *et al.*, 2003; Birnbaum *et al.*, 2004). In the past decade, great progress has been made in revealing diverse functional roles of K^+ channel subtypes in a variety of nerve cells and brain regions (reviewed by Migliore & Shepherd, 2002; Frick & Johnston, 2005), some of which require a non-homogeneous somato-dendritic channel distribution. In parallel with theoretical and functional works, immunohistochemical studies have demonstrated complex and highly regulated subcellular distribution patterns for several K^+ channel subunits. The first demonstration of localized enrichment of K^+ channels was published more than a decade ago (Laube *et al.*, 1996). Laube et al. (1996) used electron microscopic (EM) immunogold localizations to show that Kv1.1 and Kv1.2 subunits were enriched in septate-like junctions between cerebellar basket cell axons. Cooper et al. (1998) reported patchy immunolabeling for the Kv1.4 subunit in some hippocampal glutamatergic axon terminals and pre-terminal axons. Recently, a number of studies reported the postsynaptic clustering of many different K^+ channel subunits. For example, clusters of the Kv2.1 subunit were found in α-motoneurons of the spinal cord facing cholinergic and glutamatergic axon terminals (Muennich & Fyffe, 2004). Postsynaptic enrichment of the Kv4.2 subunit was reported in the supraoptic nucleus (Alonso & Widmer, 1997), developing cerebellum (Shibasaki *et al.*, 2004), visual cortex (Burkhalter *et al.*, 2006) and subiculum (Jinno *et al.*, 2005), whereas non-synaptic punctuate labeling was found in the hippocampus proper (Jinno *et al.*, 2005). In addition, the presence and dynamic regulation of non-synaptic clusters of Kv2.1 channels has been shown in hippocampal pyramidal neurons (Misonou *et al.*, 2004). Recently, we also reported the clustering of Kv4.2 and Kv4.3 subunits in junctions that do not show any morphological or molecular feature of chemical and electrical synapses (Kollo *et al.*, 2006). These results, taken together, unequivocally demonstrate the uneven, clustered cell surface distribution of several voltage-gated K^+ channel subunits. However, the question of whether the clustering occurs in postsynaptic specializations of chemical synapses or in non-synaptic junctions remains controversial.

The presence of A-type K^+ channel subunits Kv4.2 and Kv4.3 has been demonstrated in the main olfactory bulb (MOB) by means of *in situ* hybridization (Serodio & Rudy, 1998); however their precise cellular and subcellular locations remain elusive. The aim of the present study was to analyze the distribution of these subunits in the rat MOB at high resolution and to investigate whether they are evenly distributed on the somato-dendritic surface or an uneven distribution could expand the way in which they affect neuronal computation.

Materials and Methods

Tissue preparation

Male Wistar rats (27–87 days old), wild type and GAD67-GFP (Δneo) C57BL mice (Tamamaki *et al.*, 2003; generous gift from Prof. J.-M. Fritschy) as well as wild type and Kv4.2−/− 129/SvEv mice (Guo *et al.*, 2005; generous gift from Prof. D. Johnston) were deeply anaesthetized with ketamine and xylazine in accordance with the ethical guidelines of the Institute of Experimental Medicine, Hungarian Academy of Sciences. They were perfused through the aorta with 0.9% saline for 1 min, followed by ice-cold fixatives. For immunofluorescence reactions the animals were perfused with fixatives containing 4% paraformaldehyde (PFA) and either 0% or 0.05% glutaraldehyde (GA) made up in 0.1 M phosphate buffer (pH=7.4; PB) for 15-25 min. For pre-embedding immunogold reactions and for the Kv4.2-GABA colocalization immunofluorescent experiments, rats were perfused

with fixatives containing 2% PFA and 0.1-1% GA in 0.1M sodium acetate buffer (pH=6) for 2 min followed by 1 h perfusion with 2% PFA and 0.1-1% GA in 0.1M borate buffer (pH=9). For immunogold reactions, the brains were left in the skull overnight prior to removal. Horizontal sections (60 μm thick) were cut from the olfactory bulb with a Vibratome (VT1000S; Leica Microsystems, Vienna, Austria), followed by several washes in PB. Tissues fixed with 1% GA-containing fixatives were treated with 1% sodium borohydrate in 0.1 M PB for 10 min.

Pre-embedding immunohistochemistry

Sections were blocked either in 10% normal goat serum (NGS), 1.5% bovine serum albumin (BSA) or 10% normal donkey serum (NDS) made up in Tris-buffered saline (pH=7.4; TBS). Following blocking, the sections were incubated in the solutions of the primary antibodies. They were diluted in TBS containing 1-2% NGS, BSA or NDS and 0.05% Triton X-100. Details of the primary antibodies used in the present study are provided in supplementary Table 1. Here only a list of the primary Abs is provided: mouse anti-Kv4.2, rabbit anti-Kv4.2, mouse anti-Kv4.3, rabbit anti-Kv4.3, goat anti-Kv4.3, mouse anti-calretinin, rabbit anti-calretinin, rabbit anti-parvalbumin, rabbit anti-vGluT2, mouse anti-NeuN, mouse anti-tubulin beta III, mouse anti-neurofilament 200, rabbit anti-neurofilament alpha-internexin/NF66, mouse anti-GFAP, mouse anti-RIP, mouse anti-CD11b, mouse anti-CNP, mouse anti-NG2, mouse anti-RC2 (Misson *et al.*, 1988), mouse anti-MBP and mouse anti-O1 (Espinosa de los Monteros *et al.*, 1988), rabbit anti-GFP, mouse anti-GABA (Szabat et al., 1992). After several washes, the following secondary antibodies were used to visualize the immunoreactions: Alexa488 and Alexa594-coupled donkey anti-goat, donkey anti-rabbit, goat anti-mouse and goat anti-rabbit (Invitrogen, Eugene, OR); Cy3-coupled donkey anti-mouse, donkey anti-rabbit, goat anti-rabbit; biotinylated goat anti-mouse, donkey anti-goat and donkey anti-rabbit (Jackson, West Grove, PA); 0.8 nm gold coupled goat anti-mouse and goat anti-rabbit (Aurion, Wageningen, The Netherlands). Ultra small gold particles were visualized with silver (EM-SE kit; Aurion) or gold (GoldEnhance; Nanoprobes Inc, Universal Biologicals, Cambridge, UK) enhancing kits as described by the manufacturers. In EM DAB/immunogold double reactions, the ultra small gold particles were first visualized with the gold enhancement kit followed by the DAB reaction. For visualization of biotin in immunofluorescent reactions, streptavidin-conjugated Alexa350 (Invitrogen) and Cy5 (Jackson) or Oregon Green 488 tyramide (Invitrogen) was used. Images were taken with a fluorescence microscope (BX-62; Olympus, Tokyo, Japan) equipped with a CCD camera (DP30BW; Olympus) or with a confocal laser scanning microscope (FV1000; Olympus). For some images (as indicated) in order to increase focus-depth, *Z*-plane image stacks were captured and collapsed by extended focal imaging into a single image using the software package ‘Cell’ (Soft Imaging System, Munster, Germany). All tissues for EM were treated with 0.5-2% O_sO_4, 0.5% uranyl acetate, were dehydrated and embedded into Epoxy resin (Durcupan, Fluka). Digital EM images were captured with a cooled CCD camera (Cantega; Soft Imaging System) fitted on a JEOL JEM-1011 electron microscope. Three-dimensional reconstructions were performed using the open access ‘Reconstruct’ software (Fiala *et al.*, 2002). Smoothing and final rendering of the reconstructed profiles were performed with ‘Blender’ (Blender Foundation, Amsterdam, The Netherlands).

Immunoreactivity for GABA in GCs was revealed by a preembedding method on high-glurataldehyde fixed tissue.

Control experiments

When the primary antibodies were omitted from the reactions, no specific labeling was observed. The lack of cross reactivity of the secondary antibodies in double and triple labeling experiments was consistently tested. Specificity of the immunoreactions obtained

with the rabbit anti-Kv4.2 antibodies was confirmed on brain sections of Kv4.2−/− mice (generous gift from Prof. D. Johnston).

Results

Specificity of the immunosignal obtained with anti-Kv4.2 and anti-Kv4.3 antibodies

Cellular and subcellular distributions of the A-type K^+ channel subunits Kv4.2 and Kv4.3 were studied using monoclonal and polyclonal antibodies. First, we performed control experiments ensuring that the immunosignal obtained in our reactions is due to specific antibody-antigen interactions. The specificity of anti-Kv4.2 subunit immunolabeling was tested with two methods. First, double immunofluorescent reactions were carried out with two anti-Kv4.2 antibodies (Kv4.2-M and Kv4.2-R) raised against different, non-overlapping epitopes of the protein (Fig. 1A). The two antibodies labeled the same cells and subcellular structures, indicating the specificity of the labeling. For further verification of the specificity, experiments were performed with the polyclonal anti-Kv4.2 (Kv4.2-R) antibody on brain sections of Kv4.2−/− mice (Fig. 1B). The labeling pattern in control mice was very similar to that obtained in rats. The disappearance of the labeling in Kv4.2−/− mice demonstrates that all signals obtained under our experimental conditions were due to specific antibody-Kv4.2 subunit interactions. The specificity of the anti-Kv4.3 reactions was demonstrated by performing double and triple labeling experiments with two polyclonal antibodies raised against different, non-overlapping epitopes (Kv4.3-R and Kv4.3-G) and a monoclonal anti-Kv4.3 antibody (Kv4.3-M) raised against a fusion protein that partially overlaps with the epitopes of the two polyclonal antibodies. The identical labeling achieved in triple labeling experiments (Fig. 1C) established the specificity of the immunosignal obtained under our experimental conditions. A specificity test with the monoclonal anti-Kv4.3 antibody was also carried out in a previous study (Burkhalter et al., 2006) using Kv4.3−/− mice.

When immunoreactions for Kv4.2 and Kv4.3 subunits were analyzed at low magnifications, immunolabeling was found in all layers of the MOB with subunit-specific laminar and cellular labeling patterns (Fig. 1). The strongest labeling for the Kv4.2 subunit (Fig. 1A) was observed in the granule cell layer (GCL) and external plexiform layer (EPL). In addition, a small number of immunoreactive cells was apparent in the glomerular layer (GL). For the Kv4.3 subunit, the strongest labeling was seen in the GL, whereas the GCL and EPL showed moderate immunoreactivity (Fig. 1C).

Distribution of the Kv4.2 and Kv4.3 subunits in the granule cell layer

In the GCL, intense immunolabeling for the Kv4.2 subunit was found on the cell bodies and apical dendrites of a subpopulation of granule cells (GC; Fig. 2A). At higher magnifications, the inhomogeneous labeling of these cells was apparent; only parts of the somatic and dendritic membranes were strongly labeled. Such strongly immunopositive clusters (variable in size, many μm in diameter) consisted of small, intense puncta (Fig. 2C, D) the size of which (0.2-1 μm) was close to the resolution of the light microscope (LM). The proportion of GCs containing such clusters as assessed in double immunofluorescent reactions for GABA and the Kv4.2 subunit was 9.2±6.2% (n= 541 cells from randomly selected GCL areas in 4 animals). We have noticed that the intensity of GABA immunoreaction in these strongly positive cells was much lower than that found in GCs that did not contain strong Kv4.2 subunit immunopositive clusters. Antibodies against the Kv4.3 subunit also labeled a very small subpopulation of GCs that showed a partial overlap with the Kv4.2 subunit immunopositive cells (Fig. 2C). Finally, a number of large cells, which were identified as deep short-axon cells (dSACs), showed inhomogeneous labeling for the Kv4.3 subunit (Fig. 2B, D).

To gain deeper insights into the precise subcellular distribution of these subunits, EM immunogold localizations were carried out. Robust Kv4.2 subunit labeling was observed in the plasma membrane of a subset of GCs (Fig. 3A) in accordance with our LM observations. A high density of immunogold particles was consistently found in the plasma membrane at sites where a GC was in direct contact with the somata or dendrites of other GCs. Because the plasma membranes of both GCs were strongly immunopositive for the Kv4.2 subunit at these locations, we termed such specializations as 'symmetrical' (Fig. 3B-C). The K^+ channel-rich membranes were characterized by a slight thickening, increased electron density and a rigid apposition between the two opposing plasma membranes, similar to specializations previously described in the cerebellum (Kollo et al., 2006). At these membrane specializations, no sign of i) clustering of synaptic vesicles, ii) postsynaptic specializations and iii) widening of the extracellular space was observed. Occasionally, clusters of gold particles were observed around the postsynaptic density of symmetrical, probably GABAergic synapses in GC dendrites (Fig. 3D). Three-dimensional reconstructions of GCs forming Kv4.2 subunit immunopositive specializations (Fig. 8C-D) demonstrated that immunogold particles form a complex pattern inside the conjunctions, whereas gold particles are apparently randomly distributed at a much lower density in the rest of the plasma membrane. Electron microscopic analysis of the Kv4.3 subunit reaction confirmed the LM observation of strong immunoreactivity of dSACs and a small subpopulation of GCs. Similar to the Kv4.2 subunit reactions, clusters immunoreactive for the Kv4.3 subunit were observed in specializations between GC somata (Fig. 3H). However, the intensity of the labeling was considerably lower compared to that for the Kv4.2 subunit. An elevated density of immunogold particles was detected in the plasma membranes of dSACs that were in direct contact with GC somata (Fig. 3E-G). In contrast to GC-GC specializations, no enrichment of gold particles was found in the GC plasma membrane of the dSAC-GC junctions (Fig. 3G). We refer to such junctions as 'asymmetrical'.

Distribution of the Kv4.2 and Kv4.3 subunits in the mitral cell and external plexiform layers

Moderate neuropil staining and a small number of intensely labeled cells were seen in the EPL for both subunits (Fig. 4A, B). In the Kv4.2 reactions, immunopositive GC dendrites were observed ascending from the GCL towards the glomeruli (Fig. 4A). In the mitral cell layer (MCL), Kv4.2 subunit immunopositive clusters were found between mitral cells, as described previously (Kollo et al., 2006). In several of these clusters, the Kv4.2 and Kv4.3 subunits were colocalized as revealed by double labeling experiments (Fig. 4C). In the superficial part of the EPL, distal parts of mitral cell apical dendrites were outlined by inhomogeneous labeling for both the Kv4.2 and Kv4.3 subunits (Fig. 4D, E). Previous studies demonstrated that the calcium binding protein, parvalbumin is expressed in a certain subpopulation of GABAergic interneurons of the EPL (Toida et al., 1996). Double immunofluorescent experiments revealed that the Kv4.3 subunit immunopositive cells are parvalbumin immunopositive (Fig. 4G), whereas the Kv4.2 subunit immunopositive cells belong to a neurochemically different population (Fig. 4F).

Analysis of the EM immunogold reactions revealed that mitral cell somata and lateral dendrites frequently established direct contacts with each another. In these contacts, both plasma membranes showed a high density of immunogold particles labeling the Kv4.2 subunit (Fig. 5A). These K^+ channel-rich specializations were characterized by increased electron density and rigid appositions of the plasma membranes, but a lack of synaptic vesicle clusters and postsynaptic specializations (Fig. 5A), similar to those found between GCs. Outside these specializations, the membranes of mitral cell lateral dendrites were labeled by a moderate density of gold particles. This low density, homogeneous channel distribution and the small clusters are the most likely sources of the neuropil labeling for Kv4.2 subunit seen by LM in this layer. The distal parts of mitral cell apical dendrites

appeared immunopositive in the immunofluorescent reactions. However, owing to the higher resolution of the EM, we were able to reveal that the Kv4.2 subunit positive clusters were mainly present in glial processes that surround the mitral cell apical dendrites (Fig. 5B), whereas a much lower intensity of labeling was found in the apical dendrites. At the LM level, the strongest immunosignal for the Kv4.2 subunit in the EPL was found in dendrites, which ascend from the GCL towards the glomeruli. We have found that mitral cell lateral dendrites in the EPL frequently contained Kv4.2 subunit positive clusters where they were in direct contact with GC dendrites (Fig. 5C). Following thorough analysis of the reaction we noticed that certain GC dendrites consistently displayed Kv4.2 subunit immunopositive asymmetrical junctions (Fig. 5C), whereas other granule cells did not induce clustering in the same mitral cell dendrites. The apparent strong GC dendritic labeling as observed at the LM level in the EPL is mostly attributable to clusters in the mitral cell lateral dendrites associated with a subset of GC dendrites. Similar to the observation in the GCL, occasional 'symmetrical' clusters between ascending GC dendrites were observed in the EPL as well (Fig. 5E). Specializations immunopositive for the Kv4.2 subunit were also detected between mitral cell dendrites and GC gemmules (Fig. 5D). The uneven distribution of the Kv4.2 subunit in a subset of EPL interneurons (short-axon cells) was confirmed at the EM level (Fig. 5F).

Clustered Kv4.2 subunit immunoreactivity in external tufted cells of the glomerular layer

Antibodies for the Kv4.2 subunit labeled some juxtaglomerular cells (JGCs) in the GL (Fig. 6A-B). These immunopositive JGCs had large fusiform somata with a diameter of >10 μm. Because such large cells are likely to be external tufted cells (ETCs; Pinching & Powell, 1971; Antal et al., 2006) and because ETCs express vesicular glutamate transporter 2 (vGluT2; Kaneko et al., 2002; Holderith et al., 2003; Gabellec et al., 2007), we carried out double immunofluorescent reactions to identify these Kv4.2 subunit-expressing JGCs. Our results demonstrated that vGluT2 immunopositive ETCs were decorated by strong Kv4.2 subunit immunopositive clusters (Fig. 6C, D). Next, we determined that 91±2.4% (n=3 animals, n=174 cells) of the Kv4.2 subunit immunopositive JGCs were ETCs and 82±1.5% (n=3 animals, n=161 cells) of the vGluT2 immunopositive ETCs contained somatic/proximal dendritic Kv4.2 subunit immunopositive clusters. The fluorescent clusters consisted of many strong puncta that were arranged either in spots (5-7 μm in diameter, Fig. 6B, C) or in lines (Fig. 6B). The precise subcellular distribution of the Kv4.2 subunit in ETCs was further analyzed at the EM level. The highest density of immunogold particles was found in the plasma membranes of ETCs that were in contact with periglomerular cell (PGC) somata (Fig. 7A). The relatively large apposing sheets of plasma membranes, that correspond to the 5-7 μm immunofluorescent spots, contain numerous small (~0.1-0.3 μm) strongly Kv4.2 subunit immunopositive asymmetrical specializations. We also observed clusters of gold particles between ETCs and small dendritic processes (Fig. 7B). Such overlying thin dendrites could evoke a string of K^+ channel-rich junctions in ETCs, the LM appearance of which would be linearly arranged fluorescent puncta (e.g. in Fig. 6B). In summary, Kv4.2 subunit is expressed in ETCs at high densities in many asymmetrical membrane specializations. These specializations are arranged either in spots or in lines depending whether they are associated with apposing PGC somata or dendrites, respectively. The faint labeling inside the glomeruli observed for Kv4.2 subunit at the LM level (Fig. 6A) originates from a low intensity, non-clustered labeling of mitral/tufted cell dendrites and immunopositive thin glial processes enwrapping them (Fig 7C-D).

High-density of the Kv4.3 subunit in special glial processes that surround periglomerular cells

Within the whole MOB, the most intense immunoreactivity for the Kv4.3 subunit was found in the GL, where reticular neuropil labeling and strongly labeled JGC somata were apparent

(Fig. 6E). These strongly Kv4.3 subunit immunopositive JGCs had a diameter of about 5 to 7 μm (Fig. 6E, F), indicating that they comprise a subpopulation of GABAergic PGCs. Periglomerular cells are highly heterogeneous, consisting of many functionally, morphologically and neurochemically distinct subpopulations (Kosaka et al., 1998). To identify the Kv4.3 subunit positive PGC subpopulation, we performed multiple labeling experiments for the Kv4.3 subunit and several known neurochemical markers of PGCs (calretinin (CR), tyrosine hydroxylase and calbindin D-28K). No correlation between Kv4.3 subunit immunopositive cells and those labeled for calbindin D-28K and tyrosine hydroxylase was found. However, as shown in figure 6F and G, Kv4.3 subunit immunoreactivity was often found between a CR positive and a CR negative PGC. Strong fluorescent clusters typically occupied more than half of the cell bodies. Similar to the clusters on GCs, ETCs, dSACs and mitral cells, they were built up from many small puncta. The analysis of EM immunogold reactions provided a surprising observation. Our interpretation of the fluorescent reaction was that the somatic plasma membrane of some PGCs contained many clusters of immunogold particles. In contrast, immunogold particles were present in thin glia-like processes that surrounded the somata of PGCs (Fig. 7E, F). We also noticed that gold particles were not uniformly distributed in these glia-like processes. Immunogold density for Kv4.3 subunit was much higher in the plasma membrane contacting the engulfed PGC soma than that facing the neuropil (Fig. 7E, F). These thin processes are stained faintly for CR (Suppl. Fig. 3) and can be misclassified at the LM level as cytoplasmic labeling of PGCs (Fig. 6G). Three-dimensional reconstruction of such perisomatic caps from serial EM sections provided a more compelling visualization of this finding (Fig. 8A, B). A much higher density of gold particles were seen in the membrane contacting the surrounded cell (‘contact’ on Fig. 8B) than the one facing the neuropil (‘non-contact’ on Fig. 8B). Clusters of gold particles labeling the Kv4.3 subunit were also observed on small diameter dendrites within the glomerular neuropil (Fig. 7G, H), creating the apparent reticular-like immunofluorescent labeling of the glomeruli. These dendrites established several synaptic junctions within the glomeruli, whereas they formed non-synaptic K^+ channel-rich specializations with other dendrites.

In the GL of the MOB, CR is a known marker for a subpopulation of periglomerular neurons; however the morphological features of the thin Kv4.3 subunit immunoreactive processes were more indicative of glial cells. To decide whether the cells giving rise to strongly Kv4.3 subunit immunopositive caps were glia or neurons we carried out the following experiments: First we performed multiple immunofluorescent reactions with anti-Kv4.3, anti-CR and antibodies to different neuronal and glial marker proteins. In triple immunofluorescent reactions, antibodies raised against the astrocyte marker protein GFAP (glial fibrillary acidic protein); the oligodendrocyte markers RIP, MBP (myelin basic protein), O1 and CNP (2′,3′-Cyclic nucleotide-3′-phosphohydrolase); the microglia marker OX42; the radial glial marker RC2; and the oligodendrocyte precursor marker NG2 strongly labeled different cell populations. However, no labeling was found in the cell bodies of cap-forming Kv4.3 subunit immunoreactive cells (Suppl. Fig. 1). In very few cases we observed faint GFAP labeling surrounding the calretinin positive caps. Neuronal markers NeuN, NF-H, NF-66 and β-III tubulin were also absent from these cells (Suppl. Fig. 2). The fact that most JGCs were also immunonegative for these neuronal markers calls for caution in interpreting the immunonegativity. In the next series of experiments, we performed whole-cell patch-clamp recordings (see supplementary methods) from 154 juxtaglomerular neurons (cells having their cell bodies around glomeruli) selected in an indiscriminate manner. These cells were filled with biocytin for post hoc morphological analysis. Out of these cells, 101 cells were recovered, allowing detailed morphological analysis, but none of these neurons possessed cap-like processes. For 53 recorded cells, Kv4.3 subunit and CR immunofluorescent labeling was also performed. None of the 38 recovered cells were strongly immunopositive for these molecules (Suppl. Fig. 5). These results, taken together,

indicate that these cells belong to a non-neuronal population. However, the possibility that the Kv4.3 subunit immunopositive cap-forming cells are members of a very infrequent neuronal subpopulation, and therefore not included in our sample, cannot be excluded. Next, we have performed CR immunogold labeling to analyze the ultrastructure of CR+ cells at the EM level (Suppl. Fig. 3). We compared the morphological properties of 5 randomly selected CR+ cells and 5 actively selected CR+ cells that gave rise to processes forming perisomatic caps (specially searched for) on 81±14 and 75±20 serial sections per cell, respectively. Within the serially reconstructed volume of tissue, typically only half of the somata of the periglomerular cells were present. We reasoned that because most CR+ cells are periglomerular neurons, the majority of the randomly selected cells must show the characteristic features of CR+ neurons (Suppl. Fig. 3A-D) and could form the basis of a comparison with the small subpopulation of cap-forming CR+ cells. Within this reconstructed volume, two out of the 5 randomly selected neurons had a single dendrite extending into the glomerulus (Suppl. Fig. 3A) that contained several microtubules (Suppl. Fig. 3B) and receive synapses (Suppl. Fig. 3C, D). In contrast, cap-forming CR+ cells usually had only few, short, thin processes and almost never extended into the interior of the glomerulus (Suppl. Fig. 3E-G). These processes did not contain microtubules. In a few instances, we observed membrane specializations showing ultrastructural features of chemical synapses on caps (Suppl. Fig. 3H) and on the somata of cap-forming cells. In the final series of experiments, we used transgenic animals in which GFP is expressed under the promoter of glutamic acid decarboxylase 67 (GAD67-GFP knock-in mice; Tamamaki *et al.*, 2003). A previous study using these animals has shown that the GFP positive cells are periglomerular cells of the MOB as identified with several neurochemical markers (Panzanelli *et al.*, 2007). In light of our results, we addressed the question whether all CR+ PG cells express GFP. First, we performed immunofluorescent reactions against CR in these GFP-expressing mice. We counted the number of GFP-positive cells among CR labeled PG cells in 3 animals (Suppl. Fig. 4A). Our result shows that the 93.7±1.2% (n=294 cells, n=3 animals) of CR+ PG cells express GFP, but in the remaining 6.3±1.2% of the cells GFP was undetectable. After this we performed Kv4.3 subunit labeling on GFP expressing animals to assess whether Kv4.3 subunit immunopositive caps are present in the mouse brain. Distribution of the Kv4.3 subunit in the mouse glomerular layer slightly differed from that observed in rat. Weak homogeneous labeling for Kv4.3 subunit was observed in a large proportion of the PG cells. We frequently observed strong Kv4.3 subunit labeling at contacting somatic membranes of GFP-expressing PG neurons (Suppl. Fig. 4B). Kv4.3 subunit immunopositive cap-like structures were also present in mice, although they were less frequent compared to rat sections (Suppl. Fig. 4C-D). In order to gain direct evidence that Kv4.3 subunit rich cap-forming cells are present in the mouse brain and to decide whether they express GAD67, we carried out EM double labeling experiments in which the Kv4.3 subunit was visualized with the ABC/DAB immunoperoxidase method and GFP was labeled with immunogold particles. The nuclei of GABAergic granule cells and some PG cells were strongly labeled with immunogold particles, while the nuclei of mitral cells and non-neuronal glial cells were immunonegative, demonstrating the specificity of the reaction. Confirming our LM observation, we have found GFP expressing PG cells, in which the Kv4.3 subunit was concentrated at membrane junctions made by the somatic membrane where it was in direct contact with another GFP expressing neuron (Suppl. Fig. 4E). In two cases we also found juxtaglomerular cells that extended thin, strongly Kv4.3 subunit immunopositive processes that surrounded the somata of other PG cells (Suppl. Fig. 4F). In both cases the surrounded cell was GFP immunopositive, but the cells extending the small processes were immunonegative (Suppl. Fig. 4G-H). All of these data, taken together, indicate that CR+ juxtaglomerular cells are heterogeneous and those CR+ cells that possess strongly Kv4.3 subunit immunopositive cap-like processes are likely to be non-neuronal cells.

These findings draw attention to the limitations when immunohistochemical results are interpreted based exclusively on light microscopy. In the present manuscript, detailed EM examination of the immunoreactions has revealed the erroneous LM interpretation of immunoreactions in three cases. First, one of the most prominent labeling for the Kv4.2 subunit is the dendrite-like processes in the EPL as they enter from the GCL (Fig. 4A). As GC somata are strongly Kv4.2 subunit immunopositive, the most obvious interpretation of this result is that GC dendrites contain clusters of Kv4.2 subunits. However, as shown by the EM immunogold reactions, the clusters in the EPL are not solely on GC dendrites, but are present on mitral cell dendrites that are in contact with some 'cluster inducing' granule cell dendrites (Fig. 5C). Second, the distal primary/apical dendrites of mitral cells observed at the LM level appeared as if they contained a high density of the Kv4.2 and Kv4.3 subunits (Fig. 4D-E). However, EM examination was needed again to demonstrate that the majority of the labeling originates from the few tens of nanometer-thin ensheathing glial processes (Fig. 5B). Third, a very prominent labeling for the Kv4.3 subunit was observed in the somata of some PGCs when examined at the LM level (Fig. 6F-G). Electron microscopy was needed to identify that it was not the somata of PGCs that contained a high density of Kv4.3 subunit, but that they were surrounded by a very thin glial 'cap' that expressed the K^+ channels (Fig. 7E-F). In all of these cases, the real location of the proteins was within 25 nm (~4 times the width of the plasma membrane) from the apparent location inferred from LM. Even if the currently available highest resolution LM techniques were considered (e.g. ground state depletion, stimulated emission depletion, or saturated pattern excitation microscopy), such a small distance is beyond their resolution. In summary, determining the precise cellular and subcellular distribution of any protein of interest requires consorted efforts using both light- and electron microscopy.

Discussion

Our results provide evidence for a complex, cell type-specific distribution of Kv4.2 and Kv4.3 subunits in the rat main olfactory bulb. These A-type K^+ channel subunits are unevenly distributed on the surface of a variety of cells of the olfactory bulb, including granule, short-axon, mitral, external tufted, and periglomerular neurons, as well as some cap-forming glial cells at juxtaglomerular positions (for schematic illustration see Fig. 8E and F). Clusters of K^+ channels were found in membrane specializations that did not show any of the ultrastructural features of chemical synapses. Either one or both apposing membranes of these specializations contained a high density of channels, depending on whether the junctions were formed by two different or identical cell types, respectively. We propose that the non-homogeneous cell surface distribution of A-type K^+ channels increases the computational power of individual nerve cells, and the clustering in these unique membrane specializations predicts their novel role in intercellular communication.

Clustered or uneven subcellular distributions of voltage-sensitive K^+ channels have been described in many brain areas, including the spinal cord (Muennich & Fyffe, 2004), cerebellum (Laube *et al.*, 1996; Shibasaki *et al.*, 2004; Kollo *et al.*, 2006), supraoptic nucleus (Alonso & Widmer, 1997), visual cortex (Burkhalter *et al.*, 2006), hippocampus and subiculum (Cooper *et al.*, 1998; Misonou *et al.*, 2004; Jinno *et al.*, 2005; Kollo *et al.*, 2006, Bourdeau et al., 2007). Clustering was observed with LM and EM immunohistochemical methods along the somato-dendritic plasma membranes of neurons. Some studies concluded that the sites of confined channel aggregation corresponded to synaptic junctions (Alonso & Widmer, 1997; Muennich & Fyffe, 2004; Shibasaki *et al.*, 2004; Jinno *et al.*, 2005; Burkhalter *et al.*, 2006), whereas some others demonstrated that the aggregation of channels was present at sites distinct from chemical synapses (Laube *et al.*, 1996; Cooper *et al.*, 1998; Misonou *et al.*, 2004; Jinno *et al.*, 2005; Kollo *et al.*, 2006). In the present work, we also found no ultrastructural evidence for chemical synapses being the sites of Kv4.2 and Kv4.3

subunit aggregations in the MOB. The K^+ channel-rich junctions do not have presynaptic clusters of vesicles and there is no sign of pre- or postsynaptic specializations or widening of the extracellular space, which are all universal ultrastructural features of chemical synapses. This conclusion is further strengthened by our observations that K^+ channel-rich junctions are often present between cellular elements where no chemical synapse has ever been reported; e.g. between granule cell somata or between a perisomatic glial process and the enveloped neuronal soma.

A remarkable feature of the organization of the olfactory bulb granule cell layer is that the somata of GCs frequently form clusters in the neuropil, where GC somatic plasma membranes are in direct contact with each other. Clusters of the Kv4.2 (and rarely the Kv4.3) subunit were found in a number, but not all, of these contact sites. In our previous study (Kollo *et al.*, 2006) we have described symmetrical clusters of the Kv4.2 subunit between mitral cell dendrites; in the present manuscript we have demonstrated the same phenomenon for the Kv4.3 subunit. In the medial habenular nucleus, where nerve cells of similar subtypes establish K^+ channel-rich junctions among each other, both membranes contain the Kv4.2 and Kv4.3 subunits in a symmetrical manner (Kollo *et al.*, 2006). From these observations, we propose the generalization that when membrane conjunctions are formed between the same neuronal type symmetrical K^+ channel enrichments will be found. In contrast, when conjunctions are made by cells of different types, only one membrane will contain a high density of K^+ channel subunits. Such asymmetrical specializations are found in the plasma membranes of ETCs, contacted by PGC somata and dendrites. Likewise, dSACs express high concentrations of the Kv4.3 subunit in their plasma membranes where they are in direct contact with granule cell somata, whereas the granule cell side of the same specialization does not contain the same subunit. A similar asymmetric arrangement is present between cerebellar molecular layer interneurons and climbing fibers, and between unidentified axon terminals and GABAergic interneurons of the hippocampus (Kollo *et al.*, 2006). However, the possibility is open that some other K^+ channel subunits (e.g. delayed rectifiers) are present on the other side of the specialization. Although no experimental data is currently available regarding the function of these specializations, we suggest that the asymmetry or symmetry in the K^+ channel enrichment may be paralleled by mono- or bi-directional functional interactions between the participating nerve cells

In the past decade, several studies investigated the molecular mechanisms governing the cell surface distribution of K^+ channels (reviewed by Birnbaum *et al.*, 2004). A role for the scaffolding protein PSD95 (Wong *et al.*, 2002) and the actin-binding protein filamin (Petrecca *et al.*, 2000) has been revealed in the clustering of Kv4.2 subunit-containing channels. In addition, several K^+ channel-associated proteins have been discovered, forming multiprotein complexes with the subunits of the Kv4 subfamily (An *et al.*, 2000; Rhodes *et al.*, 2004; Jerng *et al.*, 2005). One of these proteins is DPP10, a protein related to the dipeptidyl aminopeptidase CD-26, which has a role in cell adhesion. The fact that the clustering of A-type K^+ channel subunits occurs in membrane specializations (junctions) and not randomly in non-junctional plasma membranes (as does the Kv2.1 subunit) suggests a critical role for auxiliary proteins, especially those that could play a role in cell adhesion. The co-clustering of K^+ channels with some auxiliary proteins that could directly or indirectly span the extracellular space, and therefore signal some aspect of the connected cell's activity, opens up the possibility that the clustered channels are differentially regulated compared to the ones that are present at a low density in the non-junctional plasma membrane.

A remarkable result of our present experiments is the cell contact-dependent concentration of the Kv4.2 and Kv4.3 subunits in glial processes. Almost 40 years ago, Price and Powell (1970) demonstrated that the apical/primary dendrites of mitral cells are surrounded by glial

lamellae. Here we have shown that these glial processes contain immunoreactive Kv4.2 and Kv4.3 subunits at a high concentration. Probably an even more surprising finding is the very high density of the Kv4.3 subunit in perisomatic cap-like glial processes in the glomerular layer. To our knowledge, our present work provides the first description of such glial caps and here we provide evidence for the enrichment of the Kv4.3 subunit in these processes. The amazing segregation of these K^+ channels between the two glial membranes (the one contacting the PGC vs. the one facing the neuropile) is one of the most remarkable examples of subcellular compartmentalization of ion channels. The two plasma membrane segments of the same process are within a few tens of nanometers and yet K^+ channels are only clustered in the one that is in direct contact with the surrounded PGC. The functional role of these channels is as yet unknown, but they might play a role in synchronization of glial functions with neuronal activity.

Supplementary Material

Refer to Web version on PubMed Central for supplementary material.

Acknowledgments

ZN is the recipient of a Wellcome Trust Project grant, a European Commission Integrated Project grant (EUSynapse project; LSHM-CT-2005-019055) and a European Young Investigator Award (www.esf.org/euryi). The financial support from these Foundations is gratefully acknowledged. We would like to thank Dr Mark Eyre for his helpful comments on the manuscript, Drs István Katona, Emilia Madarász, Peter Somogyi, Ismo Virtanen and Marija Swirtlich for antibodies and Dr László Kocsis for his help with the 3D reconstructions. We would also like to thank Prof. Jean-Marc Fritschy for perfusing GAD67-GFP mice and providing brains for our study and for Prof. Daniel Johnston for providing the Kv4.2−/− mice.

Abbreviations

BSA	bovine serum albumin
CR	calretinin
dSAC	deep short-axon cell
EM	electron microscopy
EPL	external plexiform layer
ETC	external tufted cell
GA	glutaraldehyde
GC	granule cells
GCL	granule cell layer
GL	glomerular layer
HCN	hyperpolarization activated mixed cation channel
JGC	juxtaglomerular cells
LM	light microscopy
MCL	mitral cell layer
MOB	main olfactory bulb
NDS	normal donkey serum
NGS	normal goat serum

PB	phosphate buffer
PGC	periglomerular cell
PFA	paraformaldehyde
TBS	Tris buffered saline

References

Alonso G, Widmer H. Clustering of KV4.2 potassium channels in postsynaptic membrane of rat supraoptic neurons: an ultrastructural study. Neuroscience. 1997; 77:617–621. [PubMed: 9070739]

An WF, Bowlby MR, Betty M, Cao J, Ling HP, Mendoza G, Hinson JW, Mattsson KI, Strassle BW, Trimmer JS, Rhodes KJ. Modulation of A-type potassium channels by a family of calcium sensors. Nature. 2000; 403:553–556. [PubMed: 10676964]

Antal M, Eyre M, Finklea B, Nusser Z. External tufted cells in the main olfactory bulb form two distinct subpopulations. Eur J Neurosci. 2006; 24:1124–1136. [PubMed: 16930438]

Birnbaum SG, Varga AW, Yuan LL, Anderson AE, Sweatt JD, Schrader LA. Structure and function of Kv4-family transient potassium channels. Physiol Rev. 2004; 84:803–833. [PubMed: 15269337]

Boiko T, Rasband MN, Levinson SR, Caldwell JH, Mandel G, Trimmer JS, Matthews G. Compact myelin dictates the differential targeting of two sodium channel isoforms in the same axon. Neuron. 2001; 30:91–104. [PubMed: 11343647]

Bourdeau ML, Morin F, Laurent CE, Azzi M, Lacaille JC. Kv4.3-mediated A-type K+ currents underlie rhythmic activity in hippocampal interneurons. J Neuroscience. 2007; 27:1942–1953.

Burkhalter A, Gonchar Y, Mellor RL, Nerbonne JM. Differential expression of IA channel subunits Kv4.2 and Kv4.3 in mouse visual cortical neurons and synapses. J Neurosci. 2006; 26:12274–12282. [PubMed: 17122053]

Cooper EC, Milroy A, Jan YN, Jan LY, Lowenstein DH. Presynaptic localization of Kv1.4-containing A-type potassium channels near excitatory synapses in the hippocampus. J Neurosci. 1998; 18:965–974. [PubMed: 9437018]

Espinosa de los Monteros A, Roussel G, Neskovic NM, Nussbaum JL. A chemically defined medium for the culture of mature oligodendrocytes. J Neurosci Res. 1988; 19:202–211. [PubMed: 2835492]

Fiala JC, Allwardt B, Harris KM. Dendritic spines do not split during hippocampal LTP or maturation. Nat Neurosci. 2002; 5:297–298. [PubMed: 11896399]

Frick A, Johnston D. Plasticity of dendritic excitability. J Neurobiol. 2005; 64:100–115. [PubMed: 15884001]

Gabellec MM, Panzanelli P, Sassoe-Pognetto M, Lledo PM. Synapse-specific localization of vesicular glutamate transporters in the rat olfactory bulb. Eur J Neurosci. 2007; 25:1373–1383. [PubMed: 17425564]

Guo W, Jung WE, Marionneau C, Aimond F, Xu H, Yamada KA, Schwarz TL, Demolombe S, Nerbonne JM. Targeted deletion of Kv4.2 eliminates I(to,f) and results in electrical and molecular remodeling, with no evidence of ventricular hypertrophy or myocardial dysfunction. Circ Res. 2005; 97:1342–1350. [PubMed: 16293790]

Gutman GA, Chandy KG, Adelman JP, Aiyar J, Bayliss DA, Clapham DE, Covarriubias M, Desir GV, Furuichi K, Ganetzky B, Garcia ML, Grissmer S, Jan LY, Karschin A, Kim D, Kuperschmidt S, Kurachi Y, Lazdunski M, Lesage F, Lester HA, McKinnon D, Nichols CG, O'Kelly I, Robbins J, Robertson GA, Rudy B, Sanguinetti M, Seino S, Stuehmer W, Tamkun MM, Vandenberg CA, Wei A, Wulff H, Wymore RS. International Union of Pharmacology. XLI. Compendium of voltage-gated ion channels: potassium channels. Pharmacol Rev. 2003; 55:583–586. [PubMed: 14657415]

Holderith NB, Shigemoto R, Nusser Z. Cell type-dependent expression of HCN1 in the main olfactory bulb. Eur J Neurosci. 2003; 18:344–354. [PubMed: 12887416]

Europe PMC Funders Author Manuscripts

Jenkins SM, Bennett V. Ankyrin-G coordinates assembly of the spectrin-based membrane skeleton, voltage-gated sodium channels, and L1 CAMs at Purkinje neuron initial segments. J Cell Biol. 2001; 155:739–746. [PubMed: 11724816]

Jerng HH, Kunjilwar K, Pfaffinger PJ. Multiprotein assembly of Kv4.2, KChIP3 and DPP10 produces ternary channel complexes with ISA-like properties. J Physiol. 2005; 568:767–788. [PubMed: 16123112]

Jinno S, Jeromin A, Kosaka T. Postsynaptic and extrasynaptic localization of Kv4.2 channels in the mouse hippocampal region, with special reference to targeted clustering at gabaergic synapses. Neuroscience. 2005; 134:483–494. [PubMed: 16009497]

Kaneko T, Fujiyama F, Hioki H. Immunohistochemical localization of candidates for vesicular glutamate transporters in the rat brain. J Comp Neurol. 2002; 444:39–62. [PubMed: 11835181]

Kollo M, Holderith NB, Nusser Z. Novel subcellular distribution pattern of A-type K^+ channels on neuronal surface. J Neurosci. 2006; 26:2684–2691. [PubMed: 16525047]

Kosaka K, Toida K, Aika Y, Kosaka T. How simple is the organization of the olfactory glomerulus?: the heterogeneity of so-called periglomerular cells. Neurosci Res. 1998; 30:101–110. [PubMed: 9579643]

Kulik A, Nakadate K, Hagiwara A, Fukazawa Y, Lujan R, Saito H, Suzuki N, Futatsugi A, Mikoshiba K, Frotscher M, Shigemoto R. Immunocytochemical localization of the α_{1A} subunit of the P/Q-type calcium channel in the rat cerebellum. Eur J Neurosci. 2004; 19:2169–2178. [PubMed: 15090043]

Laube G, Roper J, Pitt JC, Sewing S, Kistner U, Garner CC, Pongs O, Veh RW. Ultrastructural localization of Shaker-related potassium channel subunits and synapse-associated protein 90 to septate-like junktions in rat cerebellar Pinceaux. Molec Brain Res. 1996; 42:51–61. [PubMed: 8915580]

Lorincz A, Notomi T, Tamas G, Shigemoto R, Nusser Z. Polarized and compartment-dependent distribution of HCN1 in pyramidal cell dendrites. Nat Neurosci. 2002; 5:1185–1193. [PubMed: 12389030]

Lujan R, Albasanz JL, Shigemoto R, Juiz JM. Preferential localization of the hyperpolarization-activated cyclic nucleotide-gated cation channel subunit HCN1 in basket cell terminals of the rat cerebellum. Eur J Neurosci. 2005; 21:2073–2082. [PubMed: 15869503]

Migliore M, Shepherd GM. Emerging rules for the distribution of active dendritic conductances. Nat Rev Neurosci. 2002; 3:362–370. [PubMed: 11988775]

Misonou H, Mohapatra DP, Park EW, Leung V, Zhen D, Misonou K, Anderson AE, Trimmer JS. Regulation of ion channel localization and phosphorylation by neuronal activity. Nat Neurosci. 2004; 7:711–718. [PubMed: 15195093]

Misson JP, Edwards MA, Yamamoto M, Caviness VS Jr. Identification of radial glial cells within the developing murine central nervous system: studies based upon a new immunohistochemical marker. Brain Res Dev Brain Res. 1988; 44:95–108.

Muennich EA, Fyffe RE. Focal aggregation of voltage-gated, Kv2.1 subunit-containing, potassium channels at synaptic sites in rat spinal motoneurones. J Physiol (London). 2004; 554:673–685. [PubMed: 14608003]

Notomi T, Shigemoto R. Immunohistochemical localization of Ih channel subunits, HCN1-4, in the rat brain. J Comp Neurol. 2004; 471:241–276. [PubMed: 14991560]

Obermair GJ, Szabo Z, Bourinet E, Flucher BE. Differential targeting of the L-type Ca2+ channel α_{1C} ($Ca_V1.2$) to synaptic and extrasynaptic compartments in hippocampal neurons. Eur J Neurosci. 2004; 19:2109–2122. [PubMed: 15090038]

Panzanelli P, Fritschy JM, Yanagawa Y, Obata K, Sassoe-Pognetto M. GABAergic phenotype of periglomerular cells in the rodent olfactory bulb. J Comp Neurol. 2007; 502:990–1002. [PubMed: 17444497]

Petrecca K, Miller DM, Shrier A. Localization and enhanced current density of the Kv4.2 potassium channel by interaction with the actin-binding protein filamin. J Neurosci. 2000; 20:8736–8744. [PubMed: 11102480]

Pinching AJ, Powell TP. The neuron types of the glomerular layer of the olfactory bulb. J Cell Sci. 1971; 9:305–345. [PubMed: 4108056]

Price JL, Powell TP. The mitral and short axon cells of the olfactory bulb. J Cell Sci. 1970; 7:631–651. [PubMed: 5492279]

Rasband MN, Peles E, Trimmer JS, Levinson SR, Lux SE, Shrager P. Dependence of nodal sodium channel clustering on paranodal axoglial contact in the developing CNS. J Neurosci. 1999; 19:7516–7528. [PubMed: 10460258]

Rhodes KJ, Carroll KI, Sung MA, Doliveira LC, Monaghan MM, Burke SL, Strassle BW, Buchwalder L, Menegola M, Cao J, An WF, Trimmer JS. KChIPs and Kv4 alpha subunits as integral components of A-type potassium channels in mammalian brain. J Neurosci. 2004; 24:7903–7915. [PubMed: 15356203]

Santoro B, Grant SG, Bartsch D, Kandel ER. Interactive cloning with the SH3 domain of N-src identifies a new brain specific ion channel protein, with homology to eag and cyclic nucleotide-gated channels. Proc Natl Acad Sci U S A. 1997; 94:14815–14820. [PubMed: 9405696]

Serodio P, Rudy B. Differential expression of Kv4 K+ channel subunits mediating subthreshold transient K+ (A-type) currents in rat brain. J Neurophysiol. 1998; 79:1081–1091. [PubMed: 9463463]

Shibasaki K, Nakahira K, Trimmer JS, Shibata R, Akita M, Watanabe S, Ikenaka K. Mossy fibre contact triggers the targeting of Kv4.2 potassium channels to dendrites and synapses in developing cerebellar granule neurons. J Neurochem. 2004; 89:897–907. [PubMed: 15140189]

Szabat E, Soinila S, Happola O, Linnala A, Virtanen I. A new monoclonal antibody against the GABA-protein conjugate shows immunoreactivity in sensory neurons of the rat. Neuroscience. 1992; 47:409–420. [PubMed: 1641131]

Tamamaki N, Yanagawa Y, Tomioka R, Miyazaki J, Obata K, Kaneko T. Green fluorescent protein expression and colocalization with calretinin, parvalbumin, and somatostatin in the GAD67-GFP knock-in mouse. J Comp Neurol. 2003; 467:60–79. [PubMed: 14574680]

Toida K, Kosaka K, Heizmann CW, Kosaka T. Electron microscopic serial-sectioning/reconstruction study of parvalbumin-containing neurons in the external plexiform layer of the rat olfactory bulb. Neuroscience. 1996; 72:449–466. [PubMed: 8737415]

Trimmer JS, Rhodes KJ. Localization of voltage-gated ion channels in mammalian brain. Annu Rev Physiol. 2004; 66:477–519. [PubMed: 14977411]

Wong W, Newell EW, Jugloff DG, Jones OT, Schlichter LC. Cell surface targeting and clustering interactions between heterologously expressed PSD-95 and the Shal voltage-gated potassium channel, Kv4.2. J Biol Chem. 2002; 277:20423–20430. [PubMed: 11923279]

Europe PMC Funders Author Manuscripts

Europe PMC Funders Author Manuscripts

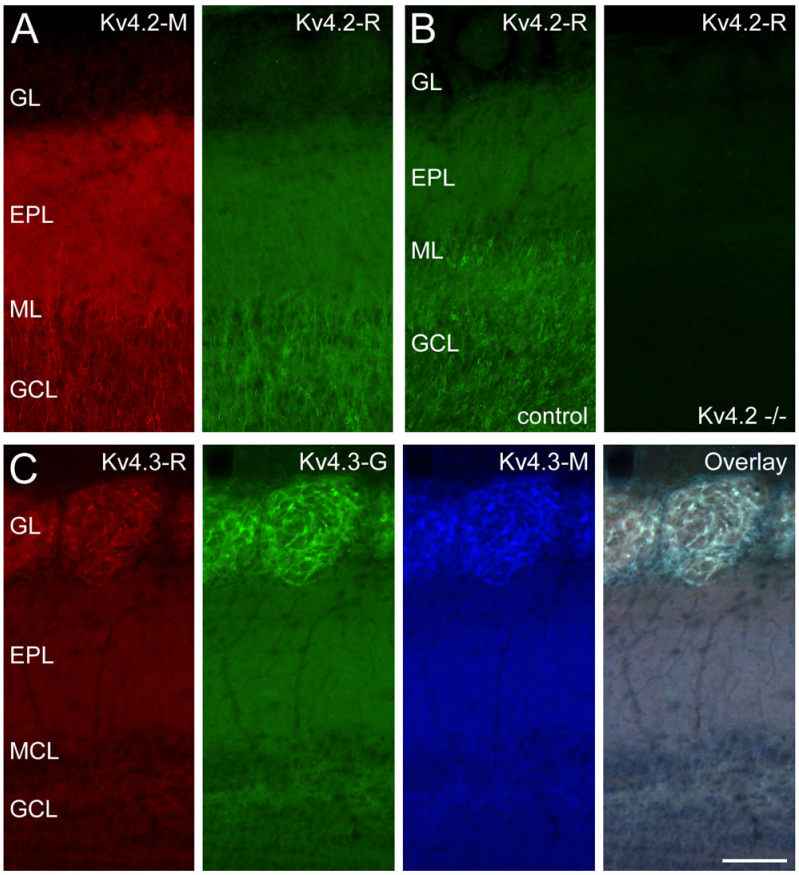

Fig. 1.

Distribution of A-type potassium channel subunits Kv4.2 and Kv4.3 in the main olfactory bulb (MOB). (A) Identical labeling was obtained with two antibodies, raised against different parts of the Kv4.2 subunit, indicating that the observed immunosignal is due to specific antibody-Kv4.2 subunit interaction. (B) No labeling was observed in Kv4.2 knockout mouse with the rabbit anti-Kv4.2 antibody, further validating the specificity of the immunoreaction. The strongest immunoreaction is seen in the granule cell layer (GCL) and external plexiform layer (EPL). (C) The specificity of Kv4.3 immunolabeling was tested by performing triple labeling experiments with three different antibodies (rabbit (R): red, goat (G): green, mouse (M): blue). The identical labeling of the MOB indicates that all signals are the consequence of specific antibody-Kv4.3 subunit interaction. The glomerular layer (GL) shows the most intense labeling for the Kv4.3 subunit. Scale bar is 100 μm and applies to all panels.

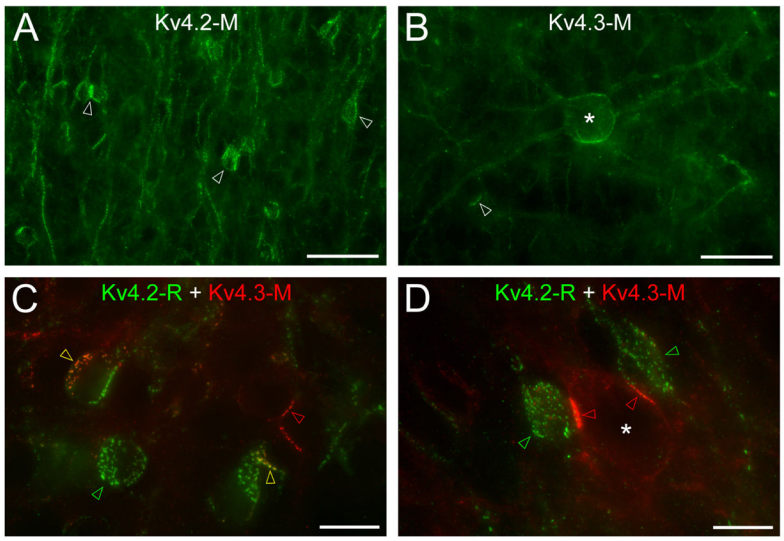

Fig. 2.

Distribution of the Kv4.2 and Kv4.3 subunits in the granule cell layer. (A) Clustered Kv4.2 subunit immunolabeling is observed in a subpopulation of granule cells (arrowheads). (B) A large deep short axon cell (*) is strongly labeled for the Kv4.3 subunit. A small number of granule cells also shows clustered labeling (arrowhead). (C) Double immunofluorescent labeling for the Kv4.2 and Kv4.3 subunits. Some granule cells express clusters of either the Kv4.2 (green arrowheads) or the Kv4.3 subunits (red arrowheads), whereas in some other granule cells Kv4.2 and Kv4.3 subunits colocalize (yellow arrowheads). (D) Strongly Kv4.3 subunit immunolabeled clusters (red arrowheads) are found in a deep short axon cell (*) close to strongly Kv4.2 subunit immunopositive granule cells (green arrowheads). Scale bars: 30 μm (A and B); 10 μm (C and D).

Europe PMC Funders Author Manuscripts

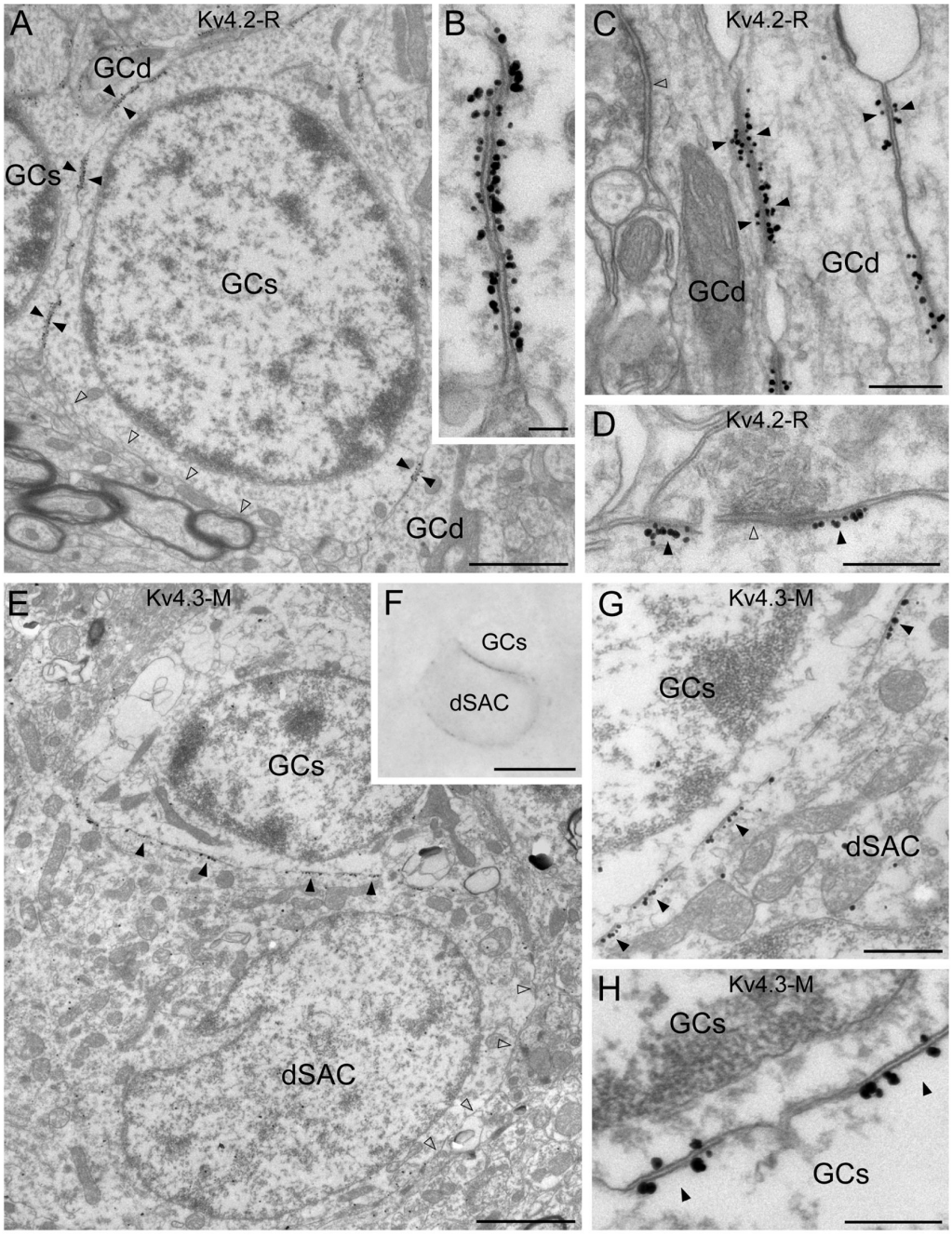

Fig. 3.

Electron microscopic immunogold localization reveals the subcellular distribution of the Kv4.2 and Kv4.3 subunits in the granule cell layer. (A) Immunogold particles for Kv4.2 subunit are clustered in membrane specializations (filled arrowheads) between granule cell somata (GCs) and dendrites (GCd). A part of the granule cell plasma membrane, which is not in direct contact with other granule cell processes (open arrowheads), contains a low density of labeling. (B) In such K^+ channel-rich specializations, both apposing granule cell membranes are strongly labeled for the Kv4.2 subunit. (C) Kv4.2 subunit immunopositive junctions (filled arrowheads) are frequently observed between granule cell dendrites (GCd) in the GCL. Open arrowhead points to a synaptic junction. (D) Clustered immunolabeling

for Kv4.2 subunit (filled arrowheads) is occasionally found around symmetrical synapses (e.g. open arrowhead) on a granule cell dendrite. (E and F) Clusters of gold particles for the Kv4.3 subunit (filled arrowheads) are observed in a deep short-axon cell (dSAC) contacting a granule cell soma (GCs). The high density of labeling is absent from other parts of the plasma membrane (open arrowheads in E). (F) Light microscopic image of the cells shown in E taken before EM sectioning. (G) A higher magnification image of the Kv4.3 subunit-rich specializations (filled arrowheads) between a dSAC and a granule cell soma (GCs). (H) Rare Kv4.3 subunit immunopositive junctions (filled arrowheads) between granule cell somata (GCs) are shown. Note that both apposing parts of the membrane specializations are labeled. Scale bars: 1.5 μm (A); 0.1 μm (B); 0.3 μm (C-E, G, H); 2 μm (E); 10 μm (F).

Europe PMC Funders Author Manuscripts

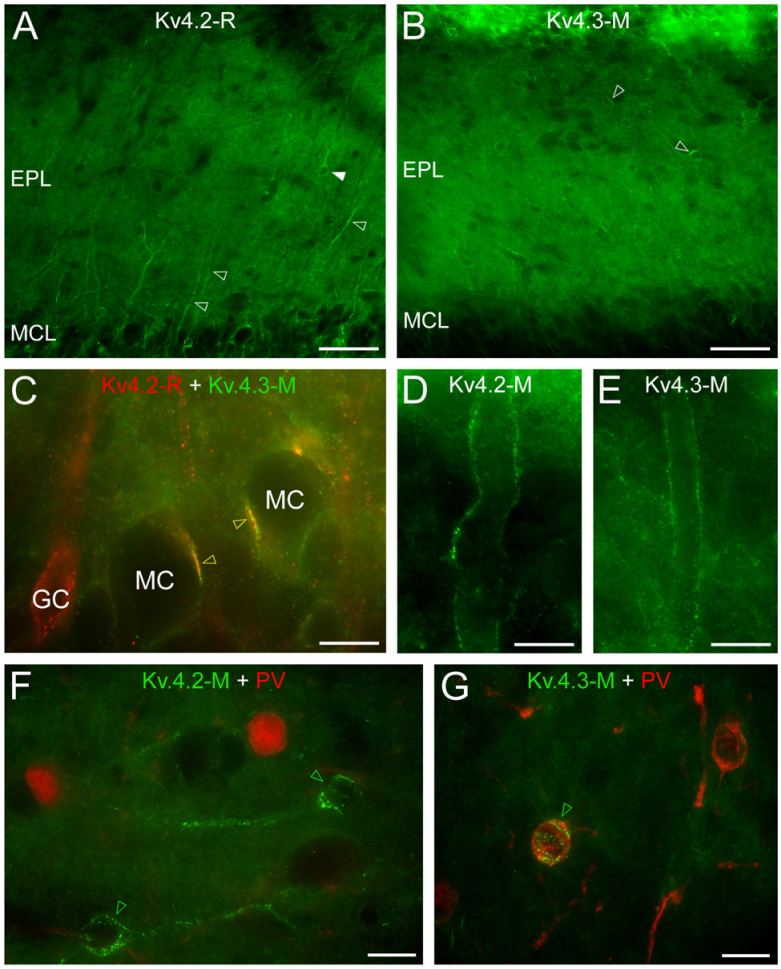

Fig. 4.

Distribution of the Kv4.2 and Kv4.3 subunits in the mitral cell and external plexiform layer. (A) Strongly Kv4.2 subunit immunolabeled dendrites (open arrowheads) dominate the homogeneous labeling of the neuropil of the external plexiform layer. A few immunopositive cell bodies are also observed (e.g. filled arrowhead) in the EPL. (B) A few Kv4.3 subunit immunopositive cell bodies (e.g. open arrowheads) stand out from the homogeneous labeling of the neuropil. (C) Double immunofluorescent labeling for the Kv4.2 and Kv4.3 subunits demonstrate their colocalization in clusters on mitral cells somata (yellow open arrowheads). (D and E) Distal parts of mitral cell apical dendrites are outlined by Kv4.2 (D) and Kv4.3 (E) subunit labeling. (F) Parvalbumin (red) immunonegative cell bodies are decorated by Kv4.2 subunit immunopositive clusters (green open arrowheads). (G) A parvalbumin immunopositive cell (green open arrowhead) of the EPL is decorated by strong Kv4.3 subunit positive clusters. Scale bars: 50 μm (A and B); 10 μm (C-G).

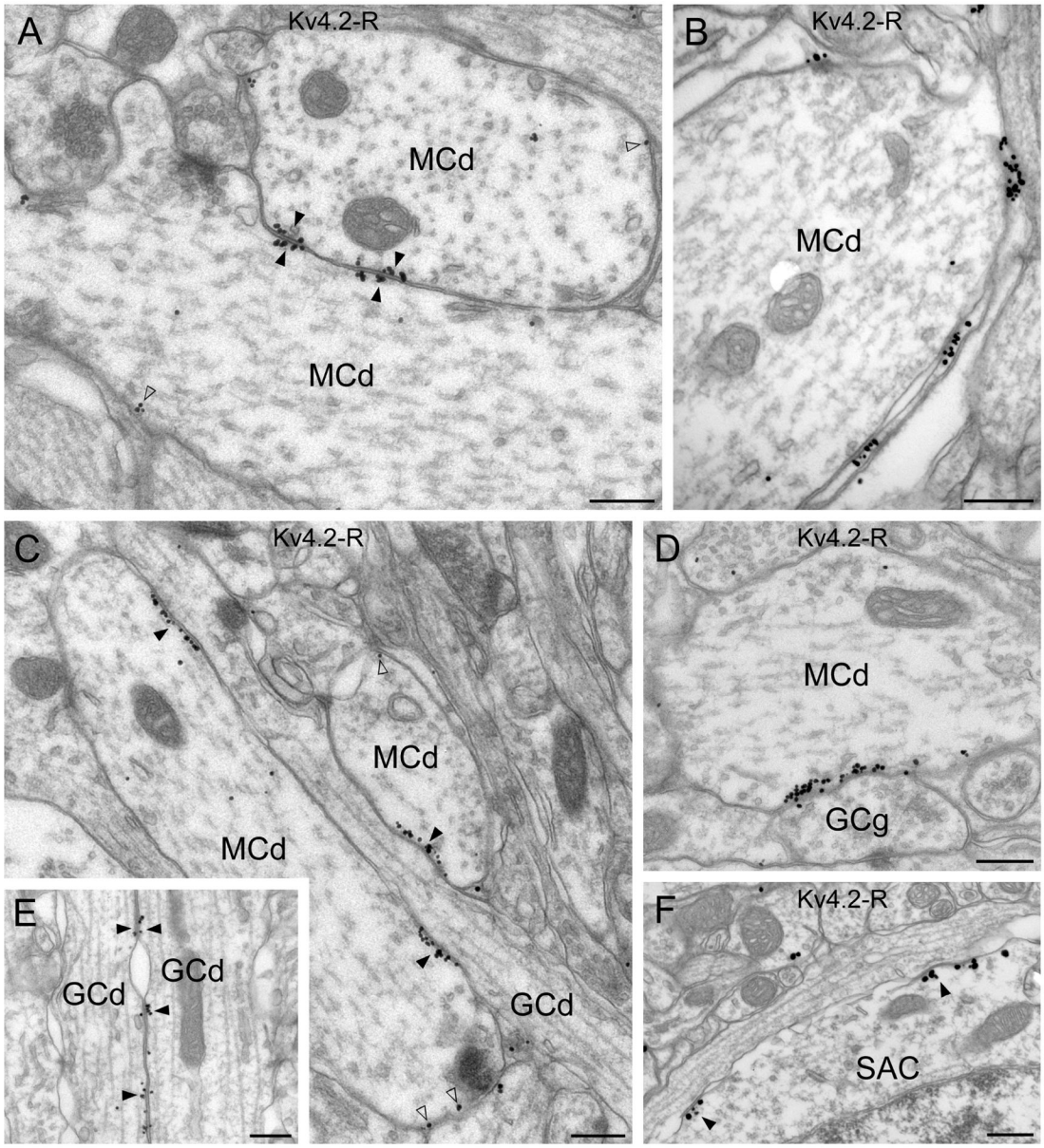

Fig. 5.

Electron microscopic immunogold localization of the Kv4.2 subunit in the mitral cell and external plexiform layers. (A) Clusters of immunogold particles for the Kv4.2 subunits are observed in membrane specializations (filled arrowheads) between two mitral cell dendrites (MCd). Note that gold particles are present in the membrane of both cells. A low intensity labeling was also found in MC lateral dendrites (open arrowheads). (B) Immunogold labeling is present in the glial sheet wrapping mitral cell apical dendrites (MCd). (C and D) A granule cell dendrite (GCd in C) and a gemmule (GCg in D) form strongly immunopositive membrane specializations with mitral cell dendrites (MCd). At these junctions, gold particles (filled arrowheads) are only found in the plasma membrane of the mitral cells. A lower density of labeling is also observed in these cells outside the specializations (open arrowheads). (E) Kv4.2 subunit immunopositive specializations are shown between granule cell dendrites (GCd) ascending into the EPL (filled arrowheads). (F)

Kv4.2 immunopositive specializations (filled arrowheads) are observed in the soma of a short axon cell (SAC). Scale bars: 0.3 μm.

Europe PMC Funders Author Manuscripts

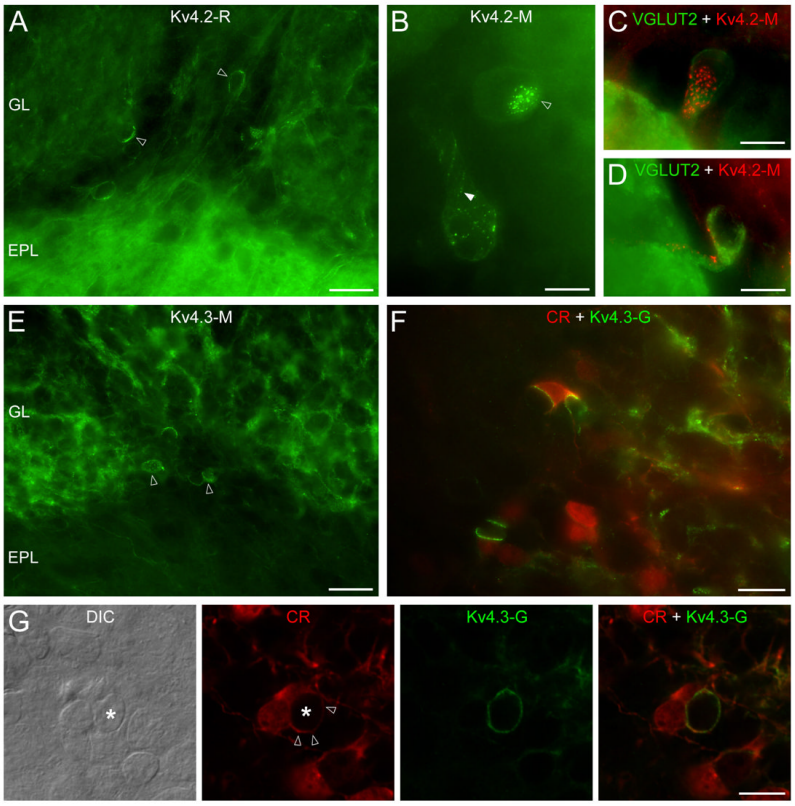

Fig. 6.

Distribution of the Kv4.2 and Kv4.3 subunits in the glomerular layer. (A) In addition to the weak neuropil labeling of the glomeruli, some juxtaglomerular cells (open arrowheads) are strongly Kv4.2 subunit immunopositive. (B) The uneven distribution of Kv4.2 subunit immunolabeling is revealed at higher magnifications. Small clusters are arranged either in disk-like (open arrowhead) or string-like (filled arrowhead) shapes. (C and D) Kv4.2 (red) subunit immunopositive cells are VGLUT2 (green) expressing external tufted cells. (E) Reticular-like labeling of the glomerular neuropil is found for the Kv4.3 subunit, in addition to a small number of immunopositive periglomerular cells (open arrowheads). (F) Double Kv4.3 subunit (green) and calretinin (CR: red) immunolabeling reveals that the intense Kv4.3 subunit clusters are often present on CR+ cells. (G) A strongly Kv4.3 subunit immunopositive process of a CR+ cell (open arrowheads) envelops another juxtaglomerular cell (*, note the nucleus on the DIC image). epifluorescent images (A and C-F); ‘extended focal image’ projection of 18 optical sections taken at 0.38 μm (B); single confocal sections (G); Scale bars: 25 μm (A and E); 20 μm (F); 10 μm (B, C, D and G).

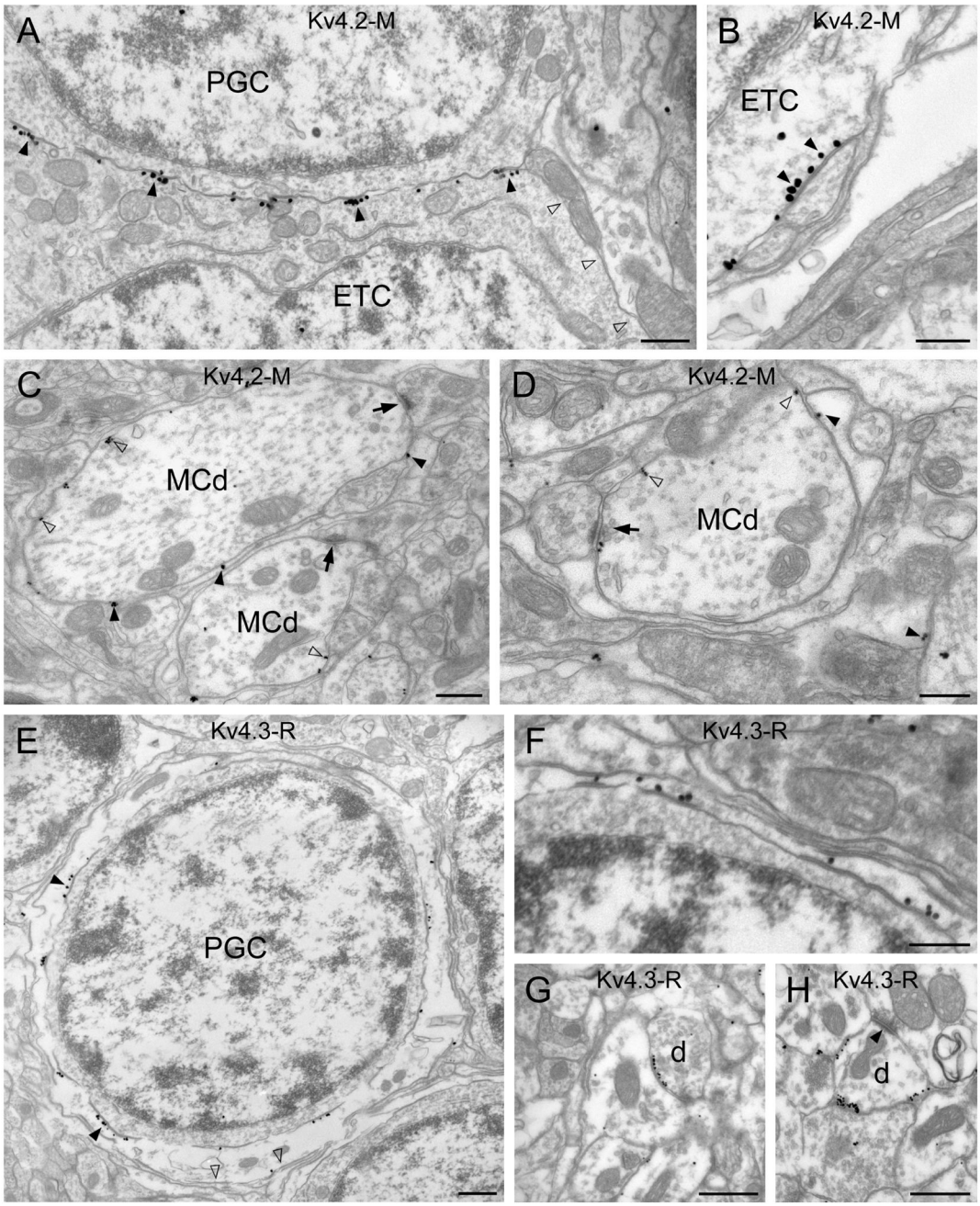

Fig. 7.

Electron microscopic immunogold localization of the Kv4.2 and Kv4.3 subunits in the glomerular layer. (A) Clusters of immunogold particles for the Kv4.2 subunit (filled arrowheads) are shown along the somatic plasma membrane of an external tufted cell (ETC) that is in direct contact with a periglomerular cell (PGC). Part of the plasma membrane that faces the neuropil (open arrowheads) is not labeled. (B) A high magnification view of an immunopositive cluster (filled arrowheads) on an ETC soma reveals that the gold particles are enriched in a membrane specialization. (C and D) Glial processes wrapping mitral/tufted cell dendrites (MCd) are labeled for the Kv4.2 subunit (filled arrowheads). A low density of labeling (open arrowheads) is found on the plasma membrane of mitral/tufted cell dendrites

(MCd), which form synapses in the glomerulus (arrows). (E) Strong immunogold labeling for Kv4.3 subunit is seen in a process enwrapping the soma of a periglomerular cell (PGC). The density of the gold particles is much higher along the membrane (filled arrowheads) that touches the PGC soma than that contacting the surrounding neuropil (open arrowheads). (F) A Kv4.3 subunit immunopositive process forms a thin sheet around a PGC. (G and H) Kv4.3 subunit positive clusters are observed on dendrites (d) in the glomerulus, which receive asymmetrical synapses (filled arrowhead) from other dendrites. Scale bars: 0.5 μm (A, C, E, G and H); 0.3 μm (B, D and F).

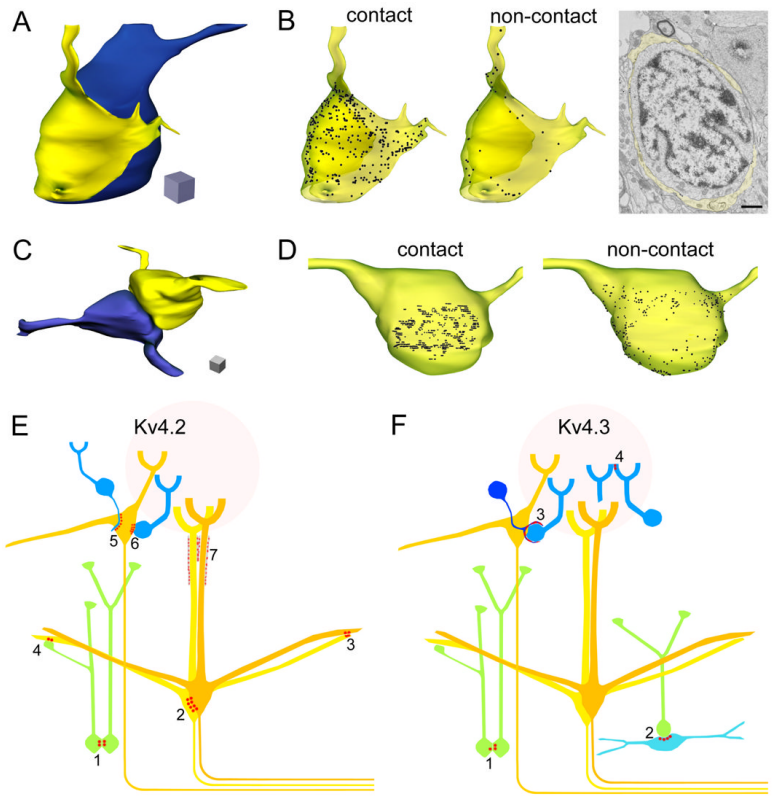

Fig. 8.

Three-dimensional reconstruction of Kv4.2 and Kv4.3 subunit immunopositive cells and schematic representation of the main cellular elements, containing K^+ channel-rich junctions. (A) 3D reconstruction of a periglomerular cell soma (blue) enwrapped by a cap-like process (yellow). (B) Distribution of the Kv4.3 subunit in the plasma membrane of the process (transparent yellow). The density of the immunogold particles on the inner membrane of the cap, contacting the cell body (contact), is much higher than that on the outer membrane (non-contact). Gold particles labeling the Kv4.3 subunit are represented as black dots. An electron micrograph from the series used for the reconstruction is shown. Scale bar: 1 μm. (C) 3D reconstruction of two granule cell somata contacting each other. (D) Distribution of the Kv4.2 subunit in the plasma membrane of one of the granule cells (yellow cell). The labeling is more intense where the cell is in contact (contact) with the other granule cell (blue cell) compared to the rest of the somatic plasma membrane (non-contact). The length of each edge of the cubes: 1 μm. (E) Schematic representation of the clustered subcellular distribution of the Kv4.2 subunit in the MOB. Clusters of the subunit were found on both sides of junctions between: somata of granule cells (green, 1), mitral cells (yellow, 2) and dendrites of mitral cells (3). Asymmetrical enrichment of the Kv4.2 subunit was observed in: mitral cells contacting granule cell dendrites (4), external tufted cells (yellow) contacting periglomerular cell (blue) dendrites (5) and somata (6). The glial sheath surrounding the distal part of the mitral cell apical dendrites also showed clustered immunolabeling (7). (F) Schematic representation of the clustered subcellular distribution of the Kv4.3 subunit. Punctuate labeling of the subunit was found in both sides of conjunctions between the somata of a small number of granule cells (1). Clusters of the subunit were observed in: a subpopulation of deep short-axon cells (light blue) contacting granule cell somata (2), processes of a gliaform juxtaglomerular cell forming perisomatic caps around periglomerular cells (3), and in periglomerular cell dendrites contacting other dendrites in the glomeruli (4).